LA-UR-97-1979

Approved for public release; distribution is unlimited

Title: **Magnet Design Concepts for the 100-MeV Isotope Production Facility**

Author(s): E. A. Wadlinger, DX-6
F. E. Merrill, LANSCE-6
J. F. Power, LANSCE-6
C. R. Rose, LANSCE-1
P. L. Walstrom, LANSCE-3

Submitted to: DOE Office of Scientific and Technical Information (OSTI)

Los Alamos
NATIONAL LABORATORY

DISTRIBUTION OF THIS DOCUMENT IS UNLIMITED

Form 836 (10/96)
ST 2629

Magnet Design Concepts for the 100-MeV Isotope Production Facility

E. A. Wadlinger*, F. E. Merrill, J. F. Power, C. R. Rose, and P. L. Walstrom

Abstract

This is the final report of a one-year, Laboratory Directed Research and Development (LDRD) project at the Los Alamos National Laboratory (LANL). The North Port Target Facility proposal includes a 100-MeV beam line to be built at the LANSCE accelerator. In developing cost and schedule estimates for this proposal, the greatest uncertainties are associated with the kicker magnet that is needed to divert portions of the beam into the new beam line. This magnet must fit into a rigidly defined space within the transition region of the existing accelerator and must operate in synchrony with the current accelerator operations systems. In addition, it must not degrade the beam quality when beam is directed to other areas of the complex. Because of these constraints the magnet must be specifically designed and built for this intended application. We have produced conceptual designs of a kicker-magnet and power supply that will meet all of the design requirements. The power supply design is based on a working design for the RIKI kicker magnet that switches 800-MeV beam into the PSR. This report presents the kicker-magnet and power-supply designs and cost and schedule estimates for incorporation into the IP facility proposal. The feasibility of various design alternatives are briefly discussed.

1. Background

We have have developed a conceptual design for a kicker magnet and power supply to be placed in the available space between QM-02 and QM-03 of the H^+ beam line in the transition region (TR) at the Los Alamos Neutron Science Center (LANSCE) accelerator (see Fig. 1) to provide beam for a proposed isotope production (IP) facility. This magnet and power supply design study shows the technical feasibility for delivering the required 100-MeV beam to the IP facility and still deliver the required beam to the Long Pulse Spallation Source (LPSS) Area-A facility, Weapons Neutron Research (WNR) facility, and Proton Storage Ring/Manual Lujan Neutron Science Center (PSR/MLNSC). We anticipate that the LPSS will require H^+ beam macropulses at 60 pulses per second (pps) and PSR will require 20 to 30 pps of H^- beam. This leaves 30 to 40 pps for other users. At the LPSS-proposed 21-mA peak H^+ beam current and 1-ms pulses, the IP facility would only need 12 pps to get the required 250 micro-amperes of beam.

---

*Principal Investigator, ewadlinger@lanl.gov

2. Beam and Beam Line Parameters

Beam optics requirements, physical size constraints, and LANSCE operational constraints determine the required kicker-magnet properties (magnet dimensions, pole tip strength, residual field, eddy current effects), and the resulting magnet design sets the magnet power-supply requirements (switching speed, voltage, current, regulation). The magnet is designed to minimize the magnetic-field energy in the gap in order to minimize the power supply requirements and minimize the time for magnet turn on and turn off. Figure 2 shows the placement of the kicker magnet in the TR.

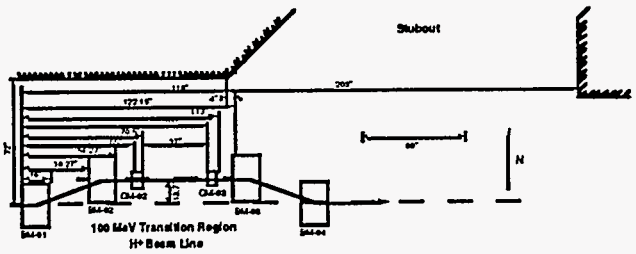

Fig. 1. LANSCE 100-MeV Transition Region showing the H^+ beam line. The kicker magnet must be placed between quadrupoles QM-02 and QM-03.

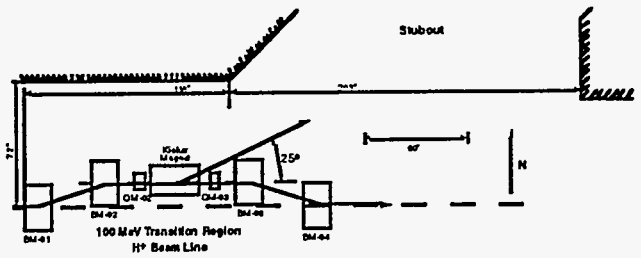

Fig. 2. LANSCE 100-MeV Transition Region showing the kicker magnet displacing the H^+ beam by 25°.

The proton energy is 100 MeV, the momentum is 444.5 MeV/c, and the magnetic rigidity is 1.48 T-m ($B\rho$). The required bend angle is approximately 25° (see Fig. 2). The total dipole-field times dipole-length product is therefore

$$Bl = \theta B\rho \tag{1}$$

which for our case is $Bl = 25^o\left(\frac{\pi}{180^o}\right)\times 1.48 = 0.65\ \text{T-m}$. The time required to establish this field is (1/120 - 0.00125) = 7 ms [120 Hz with 1.25 ms macro-pulses, see Fig. (3)] and the dipole length is ~0.8m (31.5 in). The beam pipe in the transition region is 2" OD (1.875" ID).

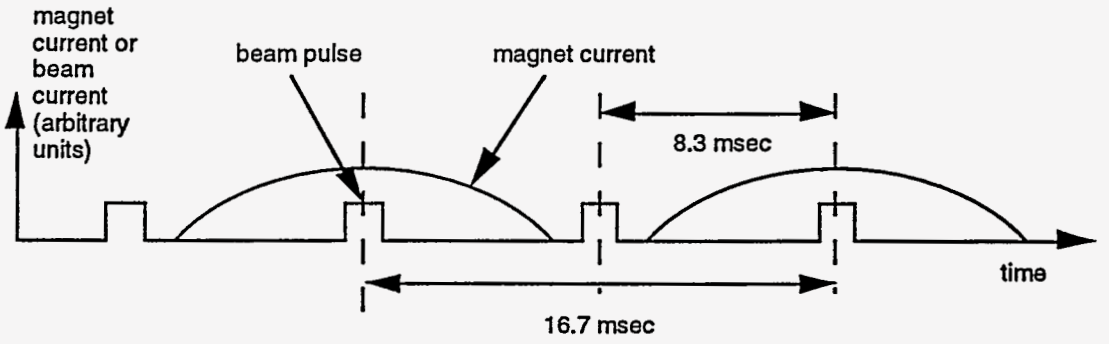

Fig. 3. LANSCE beam time structure.

The beam energy spread is ±1% or ±0.5% in momentum which requires an additional pole tip width of

$$\Delta w = \Delta\theta l = \pm 0.005 \times \frac{25^o \times \pi}{180^o} 0.8 = \pm 0.002\text{m}$$

The minimum pole tip width is therefore 5.5 cm (ignoring space for coils and additional pole tip width to achieve magnetic-field uniformity).

3. Magnet Design

The main problem is to provide a magnet that can fit into the existing space between QM-02 and QM-03, and still bend the beam enough to clear QM-03 and BM-03, the bending magnet following it. This turns out to be a bend of between 20° and 30°. The remainder of the total 45° required bend will be made with a dc magnet. The maximum fraction of macropulses extracted will be 50% (100% extraction can be achieved by driving the kicker magnet with a dc power supply). The magnet current pulse will be unipolar, as in the RIKI magnet. With the LANSCE macropulse frequency of 120 Hz, this means that the magnet pulse width can be as long as 1/60 th of a second, minus a time that includes the LANSCE macropulse time width, a flattop width, plus a design margin of about 1 millisecond. This pulse shape and width is very similar to that of the RIKI magnet. In order to lower the power-supply cost, the flattop phase of the current waveform may be eliminated and a simple half-sine-wave current pulse used. This is permissible if the resultant approximately 0.5% variation of the kick angle over the beam macropulse time width is acceptable.

The magnet yoke will be made of insulated laminations, in view of the pulsed operation. In order to minimize the pole-piece width and the stored energy, a C-shaped yoke will be used (see Fig. 4).

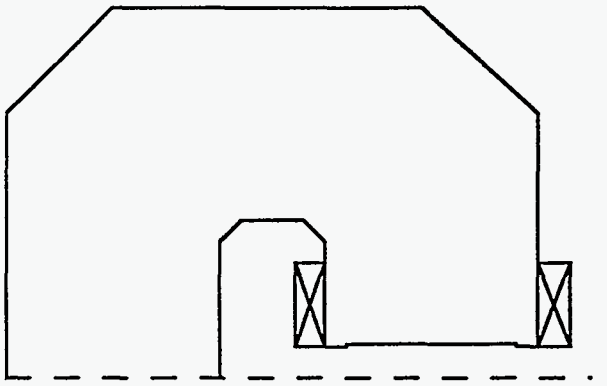

Fig. 4. Cross section of magnet yoke and windings, looking down the beamline. (not to scale).

The laminations will be staggered so that the pole faces and coils will be curved in plan view to follow the arc of the deflected beam, which will stay centered between the pole faces. The undeflected beam will pass out through the gap to the right in Fig. 4.

The pole-piece gap was chosen to accommodate a beam pipe with an outer diameter of 2 inches. A y-shaped beam pipe section will be used where the deflected and undeflected beams separate. The pole-piece width is 230 mm, or 9 inches. The gap is 2.25 in., except at the shims along the curved sides, where it is approximately 2.125 inches. Two racetrack coils with a rectangular cross section of 1 in. width and 3 in. height will be used. Two sides of the coils will be curved where they follow the curved sides of the pole pieces. Preliminary calculations with the finite-element code FLUX-2D and realistic (nonlinear) iron properties show that with a gap flux density of 1 T, the peak flux density in the yoke is 1.7 T. This represents the practical maximum flux density in high-duty-cycle pulse operation (60 Hz). The magnet could be run at somewhat higher flux density in lower-duty-cycle operation. In order to facilitate assembly (the coils will have a height that is greater than the gap), the yoke is split along the midplane on the back side. A non-metallic spacer (e.g., an epoxy-fiberglass sheet) of approximately 1/16 in. thickness will be placed in the split to ensure even flux distribution at the gap.

Preliminary magnet design parameters are given in Table 1. For example, to get the inductance per unit length, 6.32×10^{-6} is multiplied by the square of N, the number of turns. The 25°-bend case is given as an example, although, for space reasons, the 20°-bend case is more likely to be the final one chosen.

Preliminary layouts of the magnet in the beamline indicate that with a 20° bend, there will be approximately 18 cm, or 7 inches between the coil of the kicker and the yokes of the adjacent quadrupole magnets. This is enough space to accommodate field clamps of 1 in. thickness that are spaced off by 1 in. from the coils of the kicker at both ends. With this spacing, the flux density in the clamps will be approximately 0.3 T. The field clamps will be made of an epoxy-impregnated stack of the same laminations as the main yoke. This eliminates the need for a separate die for cutting the laminations of the clamps. With a coil width of 1 in., this leaves 5 in. between the clamps and the adjacent quadrupoles. This should be a sufficient distance to eliminate any significant distortion of the quadrupole field, especially by the angled clamp on the downstream end of the kicker magnet.

Table 1. Magnet Parameters

Parameter	Value
Flux density in gap	1.0 T
Inductance / (unit length-turns squared)	6.32×10^{-6} H/m
Ampere-turns at full field	4.55×10^{4} A
Stored energy at full field/unit length	6.54×10^{3} J/m
Length for 25° bend	0.65 m
Inductance for 25° bend, 20 turns	1.65×10^{-3} H
Stored energy at full field for 25° bend	4.26×10^{3} J
Current at maximum field, 20 turns	2275 A
Maximum $L\,dI/dt$ voltage for 20 turns, 25°– bend, 5.3 msec. 1/4-sine width	1104 V

With a 25° bend, the available space for a field clamp is much more limited– about 4 inches on each end. In this case, there would be approximately 2 in. clearance between the field clamp and the quadrupole yoke. There is concern about distortion of the quadrupole field in this case. If a spare quadrupole identical to QM-02 and QM-03 could be obtained, this issue could be resolved with experimental measurements with the magnet and mockup field clamps. With the 25° bend, the beam pipe of the deflected beam will clear the yokes of all of the downstream magnets. There may be interference with leads, water lines, etc., but these can be reconfigured without affecting performance. Rough layouts indicate that with 20° bend, the 2 in. beam pipe for the deflected beam will clear the yoke of the downstream quadrupole, but will "nick" the corner of the yoke of the first downstream bending magnet (BM-03) by about 1/2 in. or less. If more precise layouts of the critical region using as-built measurements confirm this, then making

such a small groove in the yoke of the magnet will have negligible effect on its performance and can probably be done *in situ* without moving the magnet.

4. Power Supply Design.

The kicker-modulator design is based on a working design now implemented with the RIKI system. This is a proven design which can be scaled to the required current level needed in the 100-MeV kicker system. The peak current is expected to be about 2300 A.

The modulator works on the principle of resonant charge. A simplified schematic is shown in Fig. 5. When fired, the pulse capacitor is discharged into the magnet through SCR1 and SCR2. The magnet inductance and selected pulse capacitance form a resonant LC circuit. When the pulse capacitor is set to a known voltage, and then discharged into the magnet, the risetime and peak magnet current are known. Just after the current peaks in the magnet in a half-sinewave, SCR3 is fired which removes the pulse capacitor from the circuit causing a flat-top or flat current response in the magnet. It is during this flat-top time period that the beam will be kicked.

The expected magnet current and voltage waveforms for this type of system are shown in Fig. 6. In the figure, the scale numbers are from the RIKI system and should be used only for representative purposes. The 100-MeV kicker will have the same type of waveshapes. The pulse flatness can be regulated to better than 1% even at 2300 A using this technique. After the flat-top portion of the cycle, SCR4 is fired which causes SCR2 to commutate, and the energy in the magnet to be dumped back into the pulse capacitor. The current in the magnet is literally reconnected electronically to the charging capacitor. Because of circuit losses, the pulse capacitor voltage won't return completely to its pre-fire initial condition. Thus, to prepare and set the proper voltage on the charging capacitor, a regulator circuit "tops off" the voltage on the capacitor after each pulse and readies it for the subsequent pulse. Referring to Fig. 6, this charge, flat-top, recovery, and top-off cycle can be done at repetition rates up to 60 Hz.

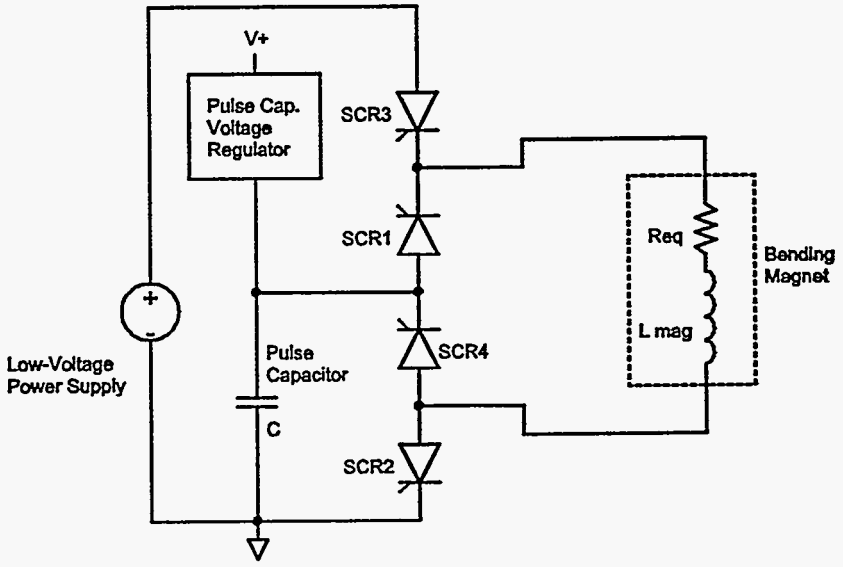

Fig. 5 Simplified schematic of the proposed 100-MeV kicker modulator.

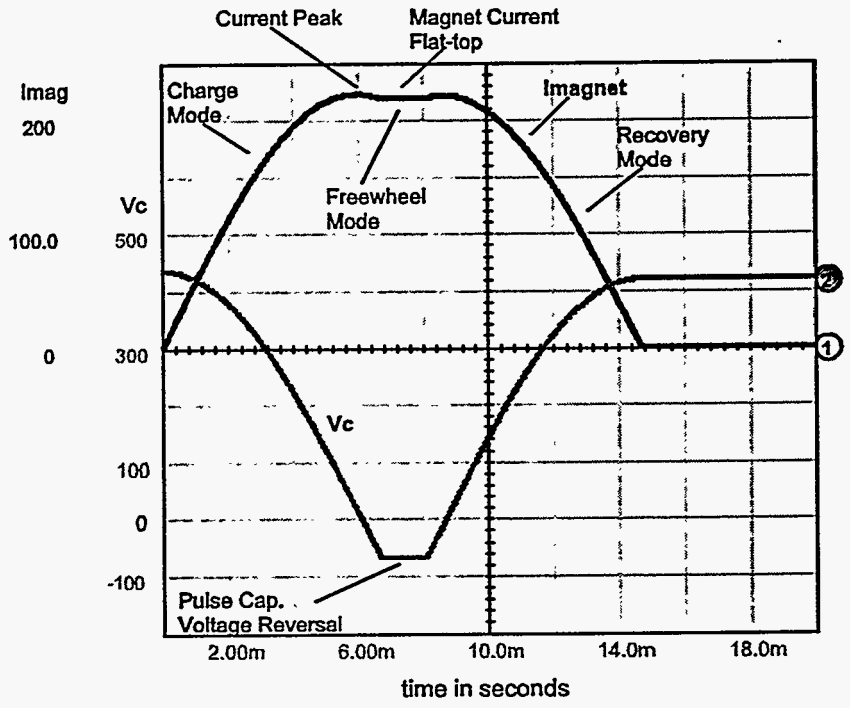

Fig. 6 Typical magnet current and pulse capacitor voltage waveforms.

This type of kicker modulator has several advantages. First it uses relatively little average power in comparison to modulators that "waste" power because this system has built-in energy recovery at the end of every pulse. Thus, even though the pulse capacitor may initially be set at 1200 VDC, and the peak current in the magnet during the pulse may be 2300 A, the average power dissipation of the system will likely be less than 10 kW. This is small in comparison to the peak power during each pulse. Second, the proposed modulator is built upon a design that is now implemented in the PSR and has worked reliably through 1 1/2 run cycles with no glitches. The proposed design will be a scale version of the existing RIKI modulator.

5. Cost and Schedule.

We estimate that the cost and effort for the magnet will be $216K for M&S, 240 hrs technician labor and 120 hrs technical staff labor. The time required to design, build, and test the magnet is approximately one year.

The total cost for the power-supply modulator is listed in Table 2. We assume that the modulator is largely designed and specified in-house, but fabricated by an outside vendor. The total LANL only costs will depend on the existing labor rates at the time of design and fabrication. Using 1996 labor rates, the estimated total cost of designing in-house and having outside fabrication is $248,800 . Estimated time for this approach is 9-10 months.

Table 2. Designed by LANL and fabricated by an outside contractor.

Labor		
design/specify system	783	Hours
test system	174	Hours
install system	261	Hours
subtotal	1218	Hours

Materials	
One kicker modulator	$120,000

6. Discussion and Summary

We have designed and costed a kicker magnet and power supply to provide 100 MeV beam for a proposed IP facility. The magnet and power supply use existing technology. The maximum magnetic field in the magnet iron is a conservative 1.7 T and the 25° bend angle is sufficient to avoid downstream magnets. However, this is not an optimized design in that we have some concern dealing with the kicker-magnetic field coupling to the adjoining quadrupoles. We could shorten the kicker magnet by increasing the magnetic field to obtain the same bend

angle, or we could reduce the bend angle to 20° and drill a hole in the yoke of BM-03 to allow the beam to pass through. These various options will be considered in the next stage of the proposal project.

We briefly considered two additional options for obtaining IP beam. One option was to use BM-02 as a kicker magnet, and the other was to place a small kicker magnet after BM-01 in the H^- beam line to minimally deflect the beam to a stripping foil placed upstream of BM-05 and use BM-05 to bend the resulting H^+ beam into a separate channel for IP. Both of these options were considered as fall back alternatives if we had difficulty with the present kicker-magnet design.

The disadvantage in using BM-02 as a kicker magnet is that the magnet must be on for H^+ beam going into the 100 - 800 MeV accelerator and off for the IP facility. Beam steering is critical for the accelerator and not critical for the IP facility. This situation should be contrasted to our proposal where the kicker magnet is off for the accelerated beam and on for the IP facility. We feel that it is easier to compensate for steering in the residual field of an off magnet than to provide superior regulation for an excited magnet.

The advantage for the kicker-magnet/stripped H^- beam system is that the kicker-magnetic field and resulting power supply requirements are minimized. However, there are two disadvantages to this scheme. One is that the H^- beam current is 1/2 that of the H^+ and significantly less current would be delivered to the IP facility. The second disadvantage is that the beam transport channel to the IP facility would be much more complicated and expensive.

APPENDIX: Useful Magnet Equations

This appendix gives the derivation of magnetic circuit equations that give a rough estimate of the magnet and power supply requirements for our application. The actual kicker-magnet design for this report was done with finite-element modeling codes that produce accurate results. However, the magnetic circuit equations provide a useful check of the modeling results and also show how parameters scale. Figure A-1 shows the dipole magnet model used to derive the magnetic circuit equations.

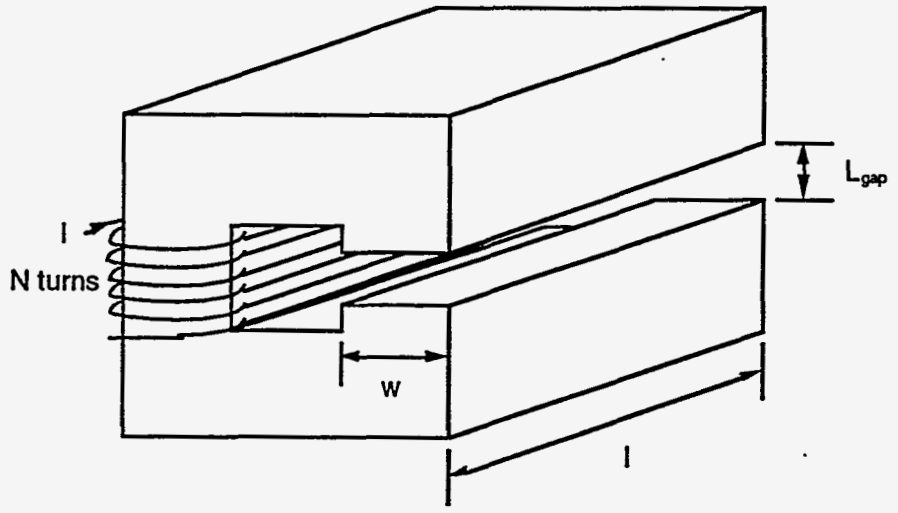

Fig. A-1. Dipole magnet used for magnetic circuit model equations.

Ampere's law plus Stokes' Theorem gives

$$\int_A \nabla \times \vec{H} \bullet d\vec{a} = \oint \vec{H} \bullet d\vec{l} = \int_A \vec{J} \bullet d\vec{a} = H_{Fe}L_{Fe} + H_{gap}L_{gap} = NI \qquad \text{(A-1)}$$

using

$$\vec{B} = \mu \vec{H} \qquad \text{(A-2)}$$

gives

$$\frac{B_{Fe}L_{Fe}}{\mu_{Fe}} + \frac{B_{gap}L_{gap}}{\mu_0} \xrightarrow{\mu_{Fe} \to \infty} \frac{B_{gap}L_{gap}}{\mu_0} = NI \qquad \text{(A-3)}$$

where $\mu_0 = 4\pi \times 10^{-7}$ and the relative permeability of iron is assumed to be infinite. From $\nabla \bullet \bar{B} = 0$, we have the continuity of the normal component of the magnetic field and therefore,

$$B_{gap} \approx B_{Fe} \approx \frac{\mu_0 NI}{L_{gap}} \tag{A-4}$$

or

$$NI = \frac{B_{gap} L_{gap}}{\mu_0} \tag{A-5}$$

Faraday's law plus Stokes' Theorem gives

$$\int_A \nabla \times \bar{E} \bullet d\bar{a} = \oint \bar{E} \bullet d\bar{l} = V_{loop} = \int_A \partial_t \bar{B} \bullet d\bar{a} \approx \partial_t \bar{B} \bullet \bar{A} \tag{A-6}$$

where V_{loop} is the electromotive force for one current loop. The electromotive force for N loops, V_N, is

$$V_N = NV_{loop} = N\partial_t \bar{B} \bullet \bar{A} = \frac{\mu_0 N^2 A}{L_{gap}} \partial_t I = L\partial_t I = NA\left(\frac{\Delta B_{gap}}{\Delta t}\right) \tag{A-7}$$

and

$$L = \frac{\mu_0 N^2 A}{L_{gap}} \tag{A-8}$$

where L is the inductance for the coil and Eq. (A-5) was used. The magnetic field-energy is

$$W_M = \tfrac{1}{2}\left[\int_{Fe} \bar{B}_{Fe} \bullet \bar{H}_{Fe}\, dv + \int_{gap} \bar{B}_{gap} \bullet \bar{H}_{gap}\, dv\right] \approx \tfrac{1}{2} \frac{B_{gap}^2 L_{gap} A}{\mu_0} = \tfrac{1}{2} \frac{\mu_0 N^2 A I^2}{L_{gap}} = \tfrac{1}{2} LI^2 \tag{A-9}$$

Combining Eqs. (A-5) and (A-7) gives the total inductive power that must be supplied to the magnet which is

$$V_N I = \frac{B_{gap} L_{gap} A}{\mu_0}\left(\frac{\Delta B_{gap}}{\Delta t}\right) = \frac{\Delta W_M}{\Delta t} \text{ (Volt - Amperes)} \tag{A-10}$$

We calculate the power supply requirements for the parameters of Sec. 2. Using the values in Sec. 2 in Eqs. (A-5), (A-7), and (A-10) gives

$$V_N I = \frac{B_{gap} L_{gap} A}{\mu_0}\left(\frac{\Delta B_{gap}}{\Delta t}\right) = \frac{0.81 \times 0.05 \times 0.8 \times 0.055}{4\pi \times 10^{-7}}\left(\frac{0.81}{7 \times 10^{-3}}\right) = 1.6 \times 10^5 \text{ (VA)} \tag{A-11}$$

$$\frac{V_N}{N} = A\left(\frac{\Delta B_{gap}}{\Delta t}\right) = 0.8 \times 0.055 \times \left(\frac{0.81}{0.007}\right) = 5.1 \text{ V} \tag{A-12}$$

$$NI = \frac{B_{gap} L_{gap}}{\mu_0} = \frac{0.81 \times 0.05}{4\pi \times 10^{-7}} = 3.2 \times 10^4 \text{ A} \tag{A-13}$$

The values in Eqs. (A-11) to (A-13) significantly underestimate the required current and voltage because the magnet size was underestimated and the field energy in the fringe field and magnet iron was neglected.